Characterization of the Depositional Conditions within the Selden Hill Through Fabric Analysis of Exposed Till

Sean Tvelia
Suffolk County Community College

Numerous studies have tried linking clast fabric strength and orientation to specific glacigenic facies. Although the data associated with these studies are tantalizing, current studies matching fabrics formed as a result of modern glaciation with ancient glacial fabric struggle to find concrete correlations. Whether or not clast fabrics accurately reflect the depositional environment or are simply an artifact of pre and post depositional processes is still greatly debated. While fabric analysis alone may not be an exact fingerprint of specific glacial processes, it remains a useful tool for identifying shear and therefore differentiating specific events and determining the relative strain involved during the deformation process of complex glacial structures. Furthermore, the resulting fabric is not only determined by the effective stress transmitted by the glacial system but by the overall rheology of the deforming sediment and, therefore, the physical conditions of the sediment at the time of final deposition.

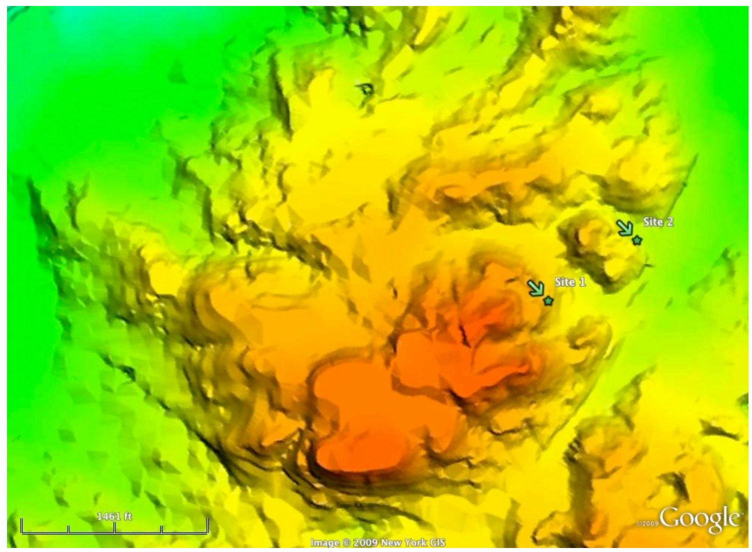

Figure 1. Digital elevation model of the Selden Hill superimposed of Google Earth globe showing scale.

The underlying principles of fabric formation, such as those described here, are based solely on the fundamental interaction of individual clasts and the applied force/stress field of an advancing glacier or ice sheet. In principle elongated clasts contained within the advancing ice or at or near the basal zone of the advancing sheet should rotate in such away as to align its major [A] axis either parallel to the directed force as described by Jeffrey (1922) or perpendicular to the directed force, which would allow rotation around the major axis as described by Taylor (1923) (Carr & Rose, 2003).

As noted by Millar (2005) the overall tendency of many similar fabric studies is to assume that once a sediment mass comes to rest, the resulting fabric is solely a record of the deformation process. While the dynamics of deformation play a crucial role in the development of clast

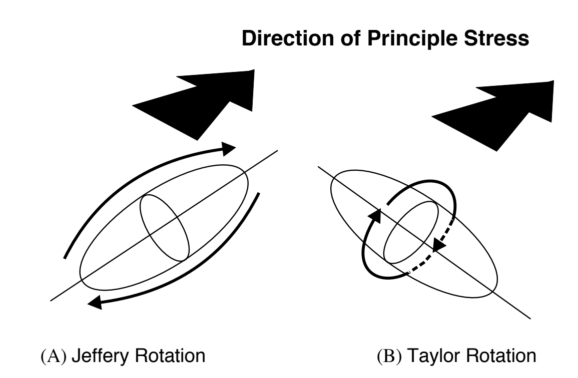

Figure 2. Particle response to directed stress as described by Jeffrey(1922) and Taylor (1923). Adapted from Carr & Rose (2003)

fabrics the mode of deposition, including clast matrix and duration of stress, may greatly affect the resulting fabric (Millar, 2005).

As shown by Glen et. al (1957) and summarized by Millar (2005) the generation of glacial fabrics may be the result of four processes: 1. the specific dynamics of the flow related to the applied stress (thickness of material and rate); 2. the individual behavior of clasts as related to their size and shape; 3. the mode of final deposition; 4. post depositional processes.

According to Carr & Rose (2003) "velocity gradients against grain surfaces cause periodic rotation of the grains into orientations parallel to the direction of the principle shear plane." Therefore the major axis of elongated clasts subjected to simple shear in periglacial environments should be oriented parallel to the direction of the local glacial advance. Hart et.al. (2009)confirm the relationship between clast orientation and glacier velocity showing that elongated probes inserted into the basal till region tended to decrease in dip during increased velocity episodes (Hart, 2009).

However, as discussed by Hart *et.al.* (2009) where the clast size is large in comparison to thickness of the shear zone, pressure-gradient driven rotation may counteract Jeffrey rotation leading to a stable clast fabric where individual clasts behave in a marker-like style as described by March (1932) and respond to original stress and then remain unchanged (Hart, 2009).

Carr & Rose (2003) also show that in studies of elongated clasts by Taylor (1923) and subsequent similar studies by Glenn (1957) the duration of the applied stress also affected clast orientation. In general these studies showed that as the duration of the applied stress increased there was a tendency for clasts to align transverse to the direction of the principal shear plane. This Taylor style orientation is further enhanced with increased matrix viscosity (Carr & Rose, 2003). Based on this it is then possible to infer duration of a deformation event based on the degree to which larger clasts have obtained a Taylor style orientation compared to that of smaller clasts.

Setting and Sedimentology

The Selden Hill is located just north of the contiguous Ronkonkoma Moraine. It reaches a maximum elevation of 245 ft above sea level at its southern boundary and descends to almost 90 ft above sea level to the north. As can be seen in the DEM in figure 1 the hill is composed of a series of concentric arcuate ridges which appear concave in the up-glacier direction. As a result of this morphology this hill has been identified as a hill-hole pair with the associated hole most likely filled during final recession and/or during a second advance which created the northern Harbor Hill Moraine.

In general these ridges (like those in similar hill-hole pairs) increase in elevation in a down-glacier direction with final and highest ridge composing the southern wall of the feature.

Borings done on the Selden Hill during construction of the Suffolk County Community College campus, which occupies the southern region of the hill, show sediment composed almost entirely of sands and gravel. Deeper Suffolk County Water Authority well logs from areas north of the Selden Hill show sediment consisting of sands and gravel, but also show an underlying clay layer which may extend beneath the Selden Hill and act as a decollement surface.

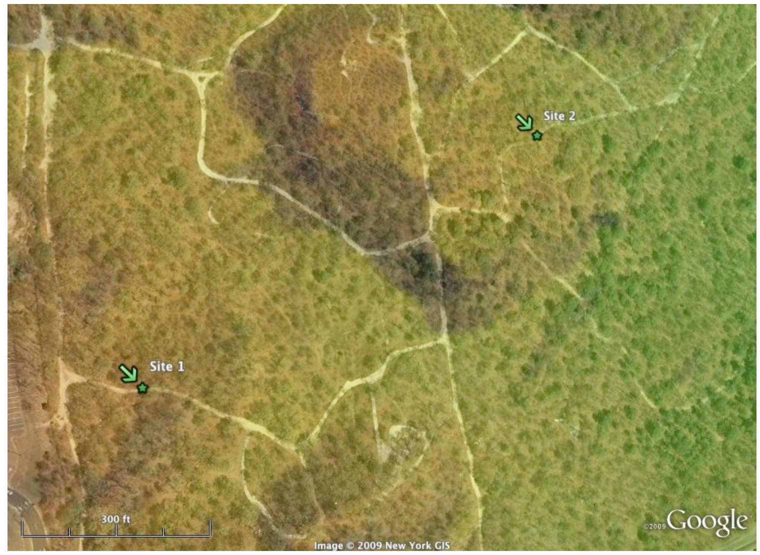

Figure 3. Arial photo of study sites. North at top of image.

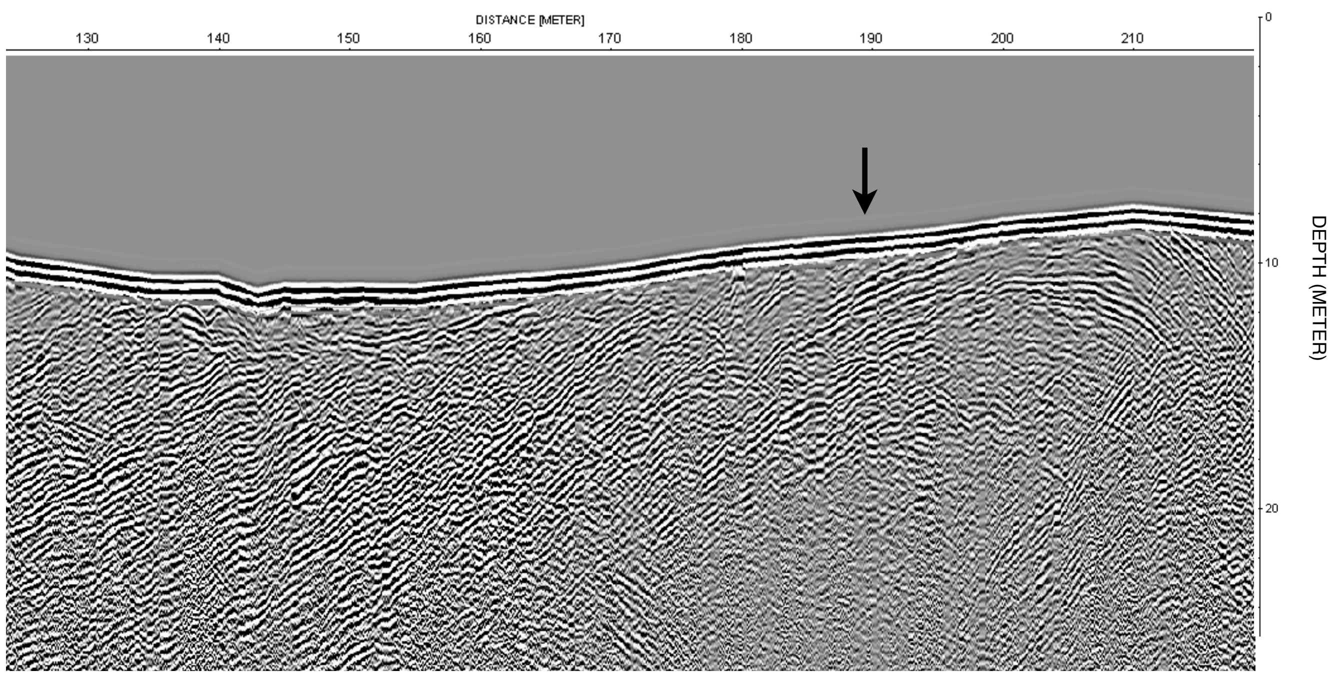

Figure 4. 200MHz GPR along north-south trail directly west of study site 1. Arrow shows position of easterly path leading to site 1.

Previous GPR studies (figure 4) of this structure show definite thrust folds all of which have been truncated at the apex; this along with a capping till suggest the entire structure had been overridden by the advancing glacier.

The presence of the deeper clay suggests that prior to the development of the Selden Hill the region north of the Ronkonkoma Moraine was most likely a glacial lake environment and may be part of the same system that produced the Smithtown Clay. The sandy texture of overlying sediment may therefore have been deposited in a Gilbert-type deltaic environment.

Site 1 is located on the eastern wall of ridge 3 (figure 3) and has local slope of 9° to the east. This site was chosen for the exposed till boundary which dips XX° to the east in an incised wall created by natural drainage and recreational ATV use. This layer is exposed on the surface just west of the site and has been imaged in previous GPR studies just east of the site where it dips below the path surface. The wall has been excavated to provide a vertical surface with an east-west strike perpendicular to the till boundary approximately 1 meter in width and 1 meter in height. Site 2 was also chosen for the convenience of an exposed till boundary along an incised wall.

Rationale and Method

The formation of hill-hole pairs have been related to the glaciotectonic thrusting of proglacial sediment. Several modern analogues of these structures have been studied and in all cases formation of these structures had been suggested to be the result of proglacial deformation caused either by englacial thrusting with subsequent deposition, by gravity spreading caused by the differential load of the ice sheet and the proglacial surface which causes thrusting of the subsurface beyond the glacial margin, or a combination of both (Andersen *et. al.,* 2005). Though clast fabric alone will not be able to differentiate between the different styles of deformation the fabric strength and clast orientation may increase our understanding of the pre and post depositional conditions required to form these structures and give greater insight into the deformational process. Specifically fabrics formed as a result of englacial thrusting and subsequent deposition may be the result of two separate stress regimes, one compressional and one extensional, where fabrics produced as a result of proglacial thrusting would be the result of compressional stresses (Carr & Rose, 2003).

Therefore in order to characterize the fabric at each site a vertical section, approximately 1 meter in width, was excavated 1.5-2 ft into the exposed wall to remove any previously slumped material and to produce an east-west vertical face exposing the buried till layer. Clasts were then carefully removed from the till as to maintain the matrix mold around the clast and the long (A), intermediate (B), and short (C) axis of each clast were measured to within 0.01 cm using vernier calipers. Then using two perpendicular rods inserted back into the original position of the clast, the bearing and plunge of both the A and B axis were measured using a Brunton pocket transit. The orientation of the C axis was then calculated based on the measured orientations of the A and

B axes. In order to minimize the error associated with the measured axis orientation, only clasts with an error of less than 10 degrees of perpendicular between their A and B axis were considered in final calculations. To account for the effect of shape on fabric development each clast was weighted such that rod-shaped clasts would be preferred over spherical clasts using a weighting factor of (A-B)/B. Out of 138 measured clast from site 1, 107 are included in the final calculations compared to 19 of the 20 clasts from site 2. Therefore, only data from site 1 meets the excepted criteria of 50 clasts for statistical

Fabric strength and orientation was then calculated via the eigenvalue method (Mark, 1974) where eigenvalues are extracted from the normalized orientation tensor represented by a symmetric 3x3 matrix of direction cosines with respect to north, east and nadir directions (l, m, n):

$$A = 1/N_{eq} \begin{vmatrix} \sum ((A_i-B_i)/B_i) l_i^2 & \sum ((A_i-B_i)/B_i)\, l_i m_i & \sum (A_i-B_i)/B_i)\, l_i n_i \\ \sum ((A_i-B_i)/B_i) l_i m_i & \sum ((A_i-B_i)/B_i)\, m_i^2 & \sum (A_i-B_i)/B_i)\, m_i n_i \\ \sum ((A_i-B_i)/B_i)\, n_i l_i & \sum ((A_i-B_i)/B_i) n_i m_i & \sum ((A_i-B_i)/B_i)\, n_i^2 \end{vmatrix}$$

$$\textit{Where } N_{eq} = \sum (A_i-B_i)/B_i$$

Resulting eigenvectors and their corresponding eigenvalues, S_1, S_2 and S_3, then represent the orthogonal axes of maximum, intermediate, and minimum clustering and the relative strengths of clustering around those axis. The strength of maximum clustering of the fabric strength is given by S_1.

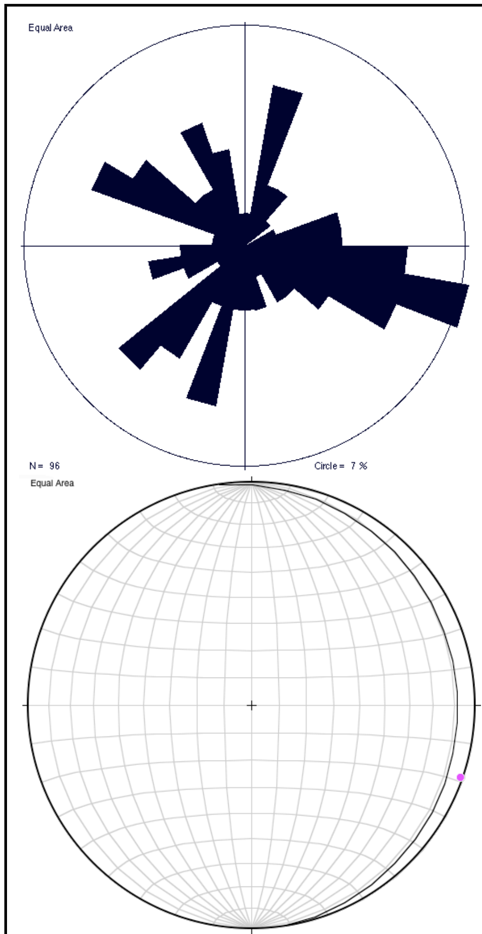

Figure 5. Top: Rose Diagram showing preferred long axial orientation of clasts at site 1. Bottom: Equal area stereonet. Arc represents plane of local slope; red dot represents principal eigenvector

Data

Eigen analysis of site 1 gives a moderately strong foliation fabric with eigenvalues of S_1= 0.47, S_2=0.38, and S_3= 0.15 with maximum clustering occurring at a bearing of 109° and plunge of 1°, as can be seen in figure 5. Site 2 results show a slightly stronger lineation with S_1= 0.59, S_2= 0.26, and S_3= 0.16 with maximum clustering occurring at a bearing of 165 degrees and plunge of 4°. Unfortunately the small number of measured clasts at this site make these results less reliable and requires further validation.

As stated previously, site 1 measurements were retrieved by excavating a vertical wall with an east-west strike, therefore any surface bias should produce fabrics with nearly north-south orientations (Klein, 2002). Eigen analysis of site 1 gives a fabric with a preferred orientation of 109°, since this is only 19° beyond the strike of the excavated surface, surface bias was most likely avoided. Site 2, in which only 19 clasts were counted in the final calculation, produced a preferred orientation of 165°. As this is nearly perpendicular to the excavated surface it is unclear whether this is a results of surface bias and needs to be verified in further studies.

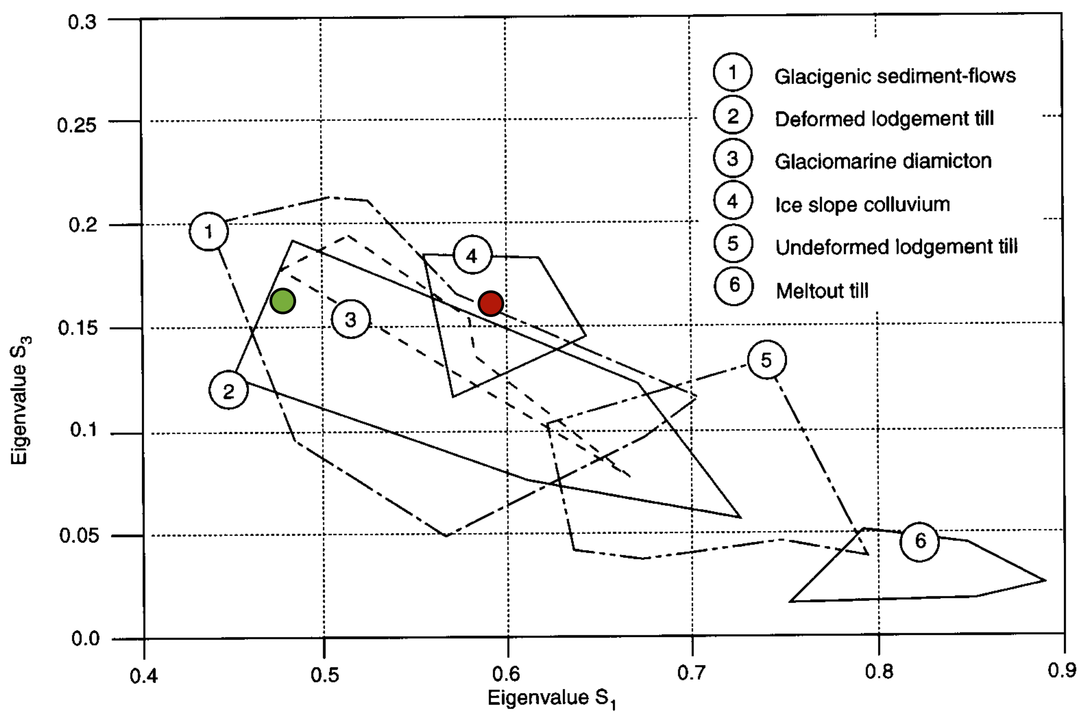

Figure 6. Process fields on bivariate eigenvalue plot adapted from Bennet 1999. Green dot showing placement of Site 1 data; Red dot showing Site 2.

Discussion

The mechanism by which deformation occurs is dependent on both the sediment deformed and its physical state; for example the presence or lack of permafrost conditions may dramatically influence the behavior of a subsurface clay boundary. Boulton *et. al.* (1999) suggest that permafrost would be essential to the deformation process, allowing the ability to transmit glacial strain over large distances and also creating elevated pore water pressure below the frost line enhancing the basal decollement surface (Boulton *et. al.* 1999).

As stated previously GPR studies conducted along the north-south path directly west of Site 1 show definite fold-thrust structures, figure 4 (Tvelia, 2007). The height of the southern most ridge (240 ft) also corresponds to the thickness of similar undeformed sediment, shown in Suffolk County Water Authority well logs, directly south of the Selden Hill. These logs also show a basal clay layer directly beneath these sediments at a depth of 240ft. It is assumed, therefore, that this clay boundary most likely acted as the basal decollement surface, which implies that initial deformation may have occurred during permafrost conditions.

The arcuate structure of the Selden Hill is similar to structures produced through deformation caused by expansion of a local dome in which clast orientation would be expected to develop a radial pattern normal to the strike of the ridge. However the width of the Selden Hill is more consistent with a local surge or ice stream than a local dome and based on this fabric orientation is expected to take on a nearly north-south orientation in the direction of the local ice movement.

The fact that site 1 data shows an orientation neither normal to the strike of the ridge or in the direction of ice flow may therefore be more indicative of the local conditions during and after deformation rather than the dynamics of the initial deformation process.

Though many studies have tried to tie fabric strength to specific glacial processes, as can be seen in figure 6, plotted eigenvalue regions typically used to describe glacial regimes often show a great deal of overlap making eigenvalues alone not a useful tool or a sole determinant of glacial processes (Bennet, 1999). However, when used alongside other evidentiary data sets, fabric analysis is still a useful tool for understanding underlying process dynamics in a given area. For purposes of this study, fabric analysis is used purely to determine the physical conditions of the deformed layer.

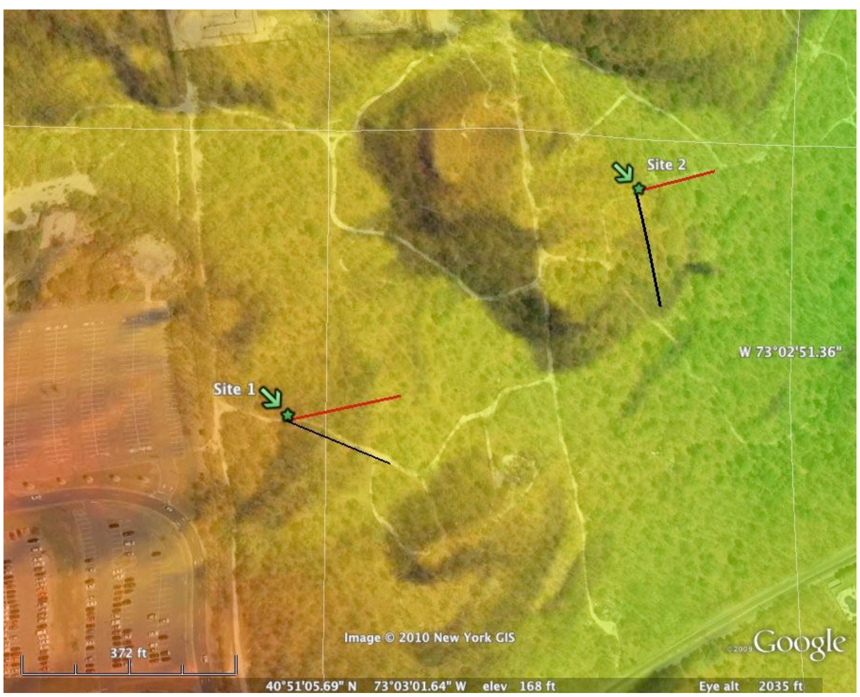

Figure 7. Hybrid DEM and arial photo showing preferred clast orientation (black) and direction of local slope (red)

Clast fabric, as recorded at site 1, shows similar patterns as those collected for deformed lodgement tills and glacigenic sediment flows, figure 6 (Bennet, 1999). Either case could potentially allow for both the fabric strength and orientation seen in this site but more interestingly this suggests, if it is not an artifact of ongoing mass wasting, that thawing not permafrost conditions were prevalent at the

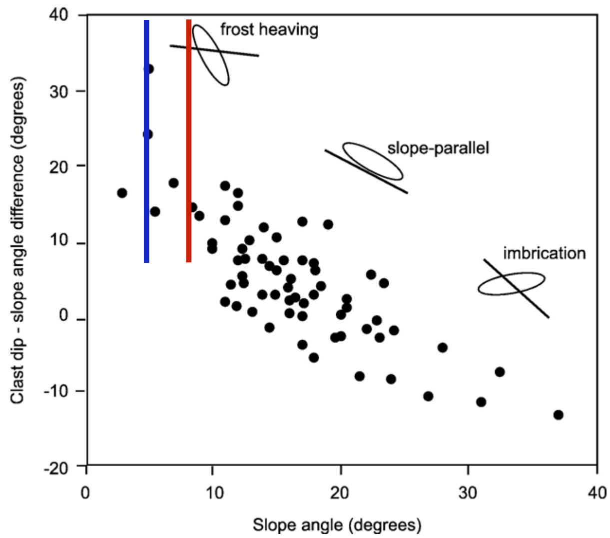

Figure 8. Adapted from Millar, 2006. Comparison of clast dip and slope angle at Eagle Summit. Red line represents range of values at site 1. Blue line represents range of values at site 2.

time of final deposition which would favor the englacial thrusting model and final deposition within a warm-base.

As can be seen in figure 7, site 1 is located on the eastward slope of a ridge; ongoing mass wasting either through slump or creep may therefore contribute to fabric development. Correlation between local slopes and fabric strength are well documented and typically show alignment with the direction of local slope (Mills, 1983; Nelson, 1985; Major, 1998; Millar, 2006). In the case of the Selden only site 1 shows a correlation between the local slope and clast orientation, figure 7.

At site 1 the local slope plunges 9° at bearing of 80° and the preferred eigenvector has a bearing of 109° and plunge of 1° given many clasts a slightly imbricated orientation with respect to the slope face. This orientation is consistent with the findings of Nelson (1985) and Mills (1983) in their studies of solifluction lobes at Eagle Summit. More recent studies at Eagle Summit by Millar (2006) also show a direct relationship between slope angle and preferred clast orientation. Millar suggests that in low angle slopes, frost heaving may be the dominant force causing clast orientations with greater dip angles than those on high angle slopes. These findings agree with those at site 1 (figure 8) suggesting that frost heaving and creep may partially responsible for the observed fabric.

Unlike site 1, site 2 shows little correlation with its local slope, as can be seen in figure 7. At site 2 the local slope dips 5° at a bearing of roughly 70°, while the preferred clast orientation dips at an angle of 3.9° at a bearing of 165°. Though individual clasts show similar dip orientations relative to the local slope as seen in site 1 suggesting that frost heaving has had considerable effect on their preferred vertical orientation, the dissimilarity between local slope bearing and long axis azimuth cannot be overlooked. Considering mass wasting processes must have been operating in this area for at least 21,000 years, if mass wasting was a factor there should be a greater correlation between the slope and the principle eigenvector as seen at Site 1. Therefore, if clast orientations are not a result of sample bias then fabric development must be a result of processes operating at the time of deposition and would favor a proglacial thrusting model. However, as stated previously, the smaller number of clasts measured at site 2 limit the reliability of these measurements and require further investigation before drawing any definitive conclusions.

Conclusion

As stated previously, past studies of the Selden Hill showed that the structure was formed through glaciotectonic processes. Furthermore, GPR images indicate that the entire structure was overridden by the advancing glacier producing the truncated folds seen in the GPR and depositing a capping till. As suggested by Boulton (1999) permafrost must be present to allow for coupling between the ice sheet and the subsurface. Permafrost condition would also cause elevated pore pressure below the frost line enhancing the separation between the deforming layers and the basal decollement surface. Using fabric analysis it may be possible to determine the presence of permafrost conditions as these conditions would directly influence the behavior of sediments during and after the deformation process. Fabric analysis of an upper till boundary located within a deformed ridge comprising the south-east wall of the Selden Hill shows sediment with an orientation that unlike the local slope and may be a result of mass wasting at the time of deformation. This would suggest a thawed sediment which may indicate that this structure was produce beneath a warm based glacier and not as a result of proglacial thrusting.

DATA: Site 1

A-Axis (cm)	B-Axis (cm)	C-axis (cm)	A-Bearing	B-bearing	A-Plunge	B-plunge
4.34	2.21	2.14	225	312	15	9
3.22	1.74	1.3	294	208	13.5	11.5
6.28	3.45	2.35	138	230	24	19
4.32	2.40	2.23	47	137	19	20
3.78	2.13	2.08	328	237	5.9	53
4.80	2.74	2.02	111	201	12	6
3.49	2.06	1.52	264	8	4.8	58
2.59	1.53	0.87	107	191	6.4	5.5
6.59	3.91	3.05	140	56	1.6	46.5
3.55	2.12	2.00	100	190	87	1.7
4.53	2.72	1.33	126	34	16.1	8
8.01	4.82	4.63	178	90	20	2
3.17	1.91	1.30	299	207	67	3
3.23	1.96	1.95	350	252	4.5	32.2
4.23	2.58	1.82	335	64	2	23
3.89	2.38	1.85	304	210	9	33
4.82	2.95	1.93	74	348	7	12.1
4.90	3.01	2.42	114	208	17.4	5
6.62	4.07	4.00	215	124	16.6	27.5
5.33	3.32	1.96	197	284	29.7	8.5
2.72	1.70	1.22	11	121	21.1	44.3
6.52	4.09	3.72	11	102	30.2	0.8
3.28	2.10	1.84	159	250	26	8.1
5.82	3.78	2.05	126	230	15	32
3.72	2.43	1.76	324	228	13.7	12.9
4.04	2.65	2.45	90	350	22.9	21.2
2.50	1.64	1.44	278	26	3.5	63.7
4.80	3.24	1.85	246	0	36.7	31.6
5.80	3.99	3.51	229	139	3	18
5.96	4.11	2.05	256	348	13	15
4.00	2.77	1.96	310	218	0.9	4.0
2.93	2.03	1.60	336	230	38.2	22.2
4.54	3.17	1.37	343	72	5	5
3.75	2.62	1.62	188	328	26.7	51.3
3.42	2.39	1.57	302	212	60.2	6.2
5.39	3.81	2.31	115	203	15	9
3.9	2.76	1.53	39	136	28	3.6
5.65	4.03	3.68	246	93	18.2	76.0
4.95	3.54	2.67	344	249	12	36

A-Axis (cm)	B-Axis (cm)	C-axis (cm)	A-Bearing	B-bearing	A-Plunge	B-plunge
3.65	2.62	2.0	294	201	13.7	5.8
6.48	4.66	3.25	216	312	20.1	14.3
6.43	4.65	4.00	122	32	4	10
4.16	3.03	1.18	96	184	21	5
2.12	1.55	1.34	162	54	36	16
4.84	3.54	2.95	68	340	2.6	72.8
3.53	2.60	1.84	25	125	4.3	47.6
2.73	2.02	1.54	198	302	23	23.8
5.60	4.15	2.87	70	170	42	4
2.67	1.98	1.62	0	270	2.2	18.0
6.75	5.01	2.53	223	116	11	39
8.59	6.38	3.68	33	304	11	25
9.00	6.69	3.07	13	282	27	10
3.85	2.87	1.56	183	94	8	9
2.89	2.16	1.51	74	168	1.5	73.2
4.13	3.09	2.50	116	212	7	26
3.19	2.41	1.45	104	356	23	36
3.40	2.57	1.49	292	193	14	21
4.08	3.09	1.94	83	175	39	6
4.53	3.46	2.16	336	231	65.1	7.7
8.82	6.78	3.63	10	100	6	37
3.65	2.82	2.23	251	341	15	19
4.29	3.33	1.33	205	114	22	4
4.48	3.48	1.87	202	296	6	8
5.23	4.08	3.10	330	64	40.5	3.4
2.73	2.13	1.32	96.5	185	12.4	1.7
4.85	3.82	2.18	306	212	11	9
4.54	3.59	1.96	100	193	44	3
7.12	5.64	2.75	317	214	22	30
2.65	2.10	1.12	90	328	30.5	46.3
3.63	2.88	1.97	305	199	42.8	12.2
6.66	5.37	2.98	232	320	1	9
3.59	2.90	2.85	344	220	66	14
3.62	2.93	1.95	104	4	33.4	6.2
4.42	3.58	2.33	88	180	21	6
7.16	5.83	4.24	224	0	22.5	63.8
3.32	2.75	1.85	87	184	43	9
3.44	2.85	1.73	28	131	13.5	64.5
3.54	2.94	1.70	178	277	22.3	7.5
2.26	1.89	1.40	264	176	2.8	26.0
6.73	5.68	3.86	130	227	19	15
4.93	4.23	1.41	280	11	7.6	5.4
4.45	3.83	2.06	96.5	191	12	20

A-Axis (cm)	B-Axis (cm)	C-axis (cm)	A-Bearing	B-bearing	A-Plunge	B-plunge
6.18	5.35	3.35	255	343	0	29
2.85	2.48	2.30	14	220	83	4
2.75	2.41	1.77	118	212	13.5	25.5
7.84	6.98	3.44	196	106	2	12
3.75	3.37	2.41	220	21	74	13
6.91	6.23	5.61	215	126	8.8	6
4.19	3.85	1.82	194	89	8	81
3.54	3.27	1.16	219	315	24	23
3.23	2.99	2.75	290	20	34	8
1.96	1.82	1.63	102	190	24.5	7.0
4.26	4.00	2.09	198	101	2.2	65.6
11.80	11.33	7.16	167	74	2	48
4.84	4.68	2.84	100	190	25	9
3.84	3.81	2.87	149	57	12.6	14.3
5.91	5.87	4.91	60	190	69.0	15.6

Data: Site 2

A-Axis	B-Axis	C-axis	A-Bearing	B-bearing	A-Plunge	B-plunge
3.84	2.72	1.91	193	291	13	36.25
5.19	3.23	2.40	144	233	11	11.5
7.95	3.69	1.73	315	52	31	12.5
3.72	2.60	1.98	145	34	40	26.5
7.41	5.75	3.41	192	282	3	32.5
5.40	4.03	2.80	164	39	15	64
3.98	3.14	1.97	250	337	4	24
2.57	1.47	1.15	304	74	67	23
3.41	2.20	2.12	174	84	26	2.5
4.03	2.27	1.88	31	171	54	29
3.80	2.08	1.47	29	121	6	67
4.12	2.28	2.08	205	290	6	2
6.06	3.52	2.41	185	102	7	18
4.80	3.01	2.08	216	309	25	12
2.92	1.69	1.14	54	143	13	9
4.57	3.18	1.40	125	35	1	30
4.15	3.01	1.73	37	162	47	18
3.92	2.95	2.14	240	114	14	69
5.80	4.08	2.50	15	108	18	13
8.69	5.41	3.40	180	269	28	2

References

Andersen, L, Hansen D., Huuse, M., 2005. Numerical Modelling of Thrust Structures in Unconsolidated Sediments: Implication for Glaciotectonic Deformation. Journal of Structural Geology 27, 587-596

Bennet, M. 2001 The Morphology, Structural Evolution and Significance of Push Moraines, Earth Science Reviews 53, 197-236

Bennet, M., Waller, R., Glasser, N., Hambrey, M., Huddart, D., 1999, Glacigenic clast fabrics: genetic fingerprint or wishful thinking?, Quarternary Science 14 (2) 125-135

Boulton, G.S., van der Meer, J.J.M., Beets, D.J. Hart, J.K., Ruegg, G.H., 1999, The Sedimentary and Structural Evolution of a Recent Push Moraine Complex: Holmstrombreen, Spitsbergen, Quaternary Science Reviews 18, 339-371

Carr, S.J., Rose, J., 2003, Till Fabric Patterns and Significance: particle response to subglacial stress. Quarternary Science reviews 22, 1415-1426

Chandler, D., Hubbard, B., 2008, Quantifying sample bias in clast fabric measurments, Sedimentology 55, 925-938

Dewen Li et.al, 2006, Fabric Analysis of Till in the Upper Urumqi River, Tiam Shan, China, Quarternary International 154-155, 19-25

Evans, D, Hiemstra, J., O'Cofaigh, C., 2007 An Assessment of Clast Macrofabrics in Glacigenic Sediments Based on A/B Plane Data, Geografiska Annaler 89-2, 103-120

Hart, J. Rose, K., Martinez, K., Ong, R., 2009, Subglacial clast behaviour and its implication for till fabric development: new results derived from wireless subglacial probe experiments, Quarternary Science Reviews 28, 597-607

Klien, E., 2002, Glaciotectonic Shear Zones: Surface Sample Bias and Clast Fabric Interpretation, Masters Thesis, Department of Earth & Space Science, Stony Brook University

Mark, David M. (1974). On the interpretation of till fabrics. Geology, 2, 101-104.

Millar, S. 2005, Fabric Variability associated with periglacial mass-wasting at Eagle Summit, Geomorphology 72, 222-237

Mills, H., 1983, Clast-Fabric Strength in Hillslope Colluvium as a Function of Slope Angle, Geografiska Annaler 65, 255-262

Nelson, F.E., 1985, A Preliminary Investigation of Solifluction Macrofabrics, Catena 12, 23-33

Tvelia, S., Characterization of the Glaciotectonic Development of the Selden Hill through Digital Elevation Models and Ground Penetrating Radar, Research Report, 2007